

# PROCEEDINGS OF SPIE

[SPIDigitalLibrary.org/conference-proceedings-of-spie](https://SPIDigitalLibrary.org/conference-proceedings-of-spie)

## Absolute polarimetric calibration of the retardance of a liquid crystal on silicon microdisplay

A. Sánchez-Montes, A. Márquez, J. Francés, F. Martínez-Guardiola, E. Calzado, et al.

A. R. Sánchez-Montes, A. Márquez, J. Francés, F. J. Martínez-Guardiola, E. M. Calzado, S. Gallego, I. Pascual, A. Beléndez, "Absolute polarimetric calibration of the retardance of a liquid crystal on silicon microdisplay," Proc. SPIE 12673, Optics and Photonics for Information Processing XVII, 126730A (4 October 2023); doi: 10.1117/12.2672547

**SPIE.**

Event: SPIE Optical Engineering + Applications, 2023, San Diego, California, United States

# Absolute polarimetric calibration of the retardance of a liquid crystal on silicon microdisplay

A. R. Sánchez-Montes<sup>1</sup>, A. Márquez\*<sup>1,2</sup>, J. Francés<sup>1,2</sup>, F. J. Martínez-Guardiola<sup>1,2</sup>, E. M. Calzado<sup>1,2</sup>, S. Gallego<sup>1,2</sup>, I. Pascual<sup>1,3</sup>, A. Beléndez<sup>1,2</sup>

<sup>1</sup>I.U. Física Aplicada a las Ciencias y las Tecnologías Universidad de Alicante, P.O. Box 99, E-03080, Alicante, Spain; <sup>2</sup>Dept. de Física, Ing. de Sistemas y Teoría de la Señal, Universidad de Alicante, P.O. Box 99, E-03080, Alicante, Spain; <sup>3</sup>Dept. de Óptica, Farmacología y Anatomía, Universidad de Alicante, P.O. Box 99, E-03080, Alicante, Spain

\*andres.marquez@ua.es

## ABSTRACT

The phase-shift exhibited by liquid crystal on silicon devices (LCoS) depends on the voltage applied and the illumination wavelength. Most of the LCoS used in the labs are digitally addressed using a binary pulse width modulated signal. Usually, these devices are characterized for a very small range of the available binary voltage values and for specific wavelengths. In this work, we consider a commercial parallel-aligned liquid crystal on silicon device (PA-LCoS) in which the binary voltages are accessible through the software of the vendor. We perform a complete averaged Stokes polarimetric characterization of the device where we are able to obtain the absolute unwrapped retardance values for a wide range of voltage parameters and across the visible spectrum. This provides a practical approach to evaluate the whole range of phase modulation possibilities, and to analyze some issues related with the physics of the device.

**Keywords:** Polarization, Liquid crystal on silicon displays, Polarimetry, Spatial light modulation, Displays

## 1. INTRODUCTION

Spatial control of light wavefronts is a very important subject, transversal to many different applications in Optics and Photonics [1-3]. Within this context, parallel-aligned liquid crystal on silicon (PA-LCoS) microdisplays is probably the most widespread spatial light modulator (SLM) device due to its high pixel number count, inherent phase-only modulation capability and high level of maturity in the technology [1-3].

PA-LCoS devices can be easily modeled as linear variable retarders [4]. However, these are complex devices, and when performing a rigorous characterization, then different non-ideal phenomena arise, mainly time fluctuations (called flicker) in digital backplane LCoS microdisplays [5-7], and pixel cross-talk effects [8-10]. Within the latter we can distinguish between fringing-field effects and vicinity effects between liquid crystal (LC) molecules [10]. Then, more accurate models, both semianalytical [4,7] and rigorous electromagnetic [10] have been proposed. Then, some of these more accurate approaches enable to characterize and computationally evaluate the phase modulation dynamic range, the associated flicker and the orientation of the LC director as a function of the applied voltage [7], and also as a function of the wavelength and the angle of incidence [11,12].

However, in general all the phase characterization approaches suffer from ambiguities due to the wrapped values that are generally obtained, since typically functions like arctangent or arccosine need to be applied to the experimental measurements [4,7]. This will introduce an ambiguity of  $360^\circ$  or  $180^\circ$  in the phase unwrapping, and the specific offset in the phase-shift needs additional knowledge or measurements to be obtained with certainty. This is important if an absolute characterization is pursued, which might be needed in some applications, as in spatial light modulation of the state of polarization (where  $180^\circ$  of ambiguity leads to confusing the slow and the fast axis of a retarder) or if we want to get a deeper insight into the details of the LC layer and analyze the thickness of the device, the aspect ratio or fill factor effects, or the influence of the applied voltage dynamic range onto the 3D LC director [10]. In this work, we show how we can obtain with certainty the absolute value of the unwrapped retardance for several illumination wavelengths and applied voltages.

## 2. HOMOGENEOUS MODELLING OF THE LC LAYER

PA-LCoS devices, especially digital backplane ones, suffer from flicker [5-7]. Polarimetric-based characterization approaches have demonstrated to be very simple and robust to characterize both the retardance and its associated flicker, when compared with diffractive-based and interferometric-based techniques [13]. At this respect, in 2014 we proposed a time-averaged Stokes polarimetric technique [4], and then in 2020 we expanded this technique so that not only retardance and flicker are measured, but also the orientation of the LC director as a function of the applied voltage [7]. In this paper we show the results when applying the latter approach [7]. In this approach, there is an ambiguity in the unwrapped retardance of  $180^\circ$ .

In Ref. [7], the Mueller-Stokes model describing the PA-LCoS shows that the output reflected Stokes vector has the following expression when impinging with right-handed circularly (RHC) polarized light,

$$S_{out} = \begin{pmatrix} S_0 \\ S_1 \\ S_2 \\ S_3 \end{pmatrix} = I_0 \begin{pmatrix} 1 \\ -\text{sinc}(a) \sin \Gamma \sin(2\theta) \\ -\text{sinc}(a) \sin \Gamma \cos(2\theta) \\ -\text{sinc}(a) \cos \Gamma \end{pmatrix} \quad (1)$$

, where  $I_o$  is the output intensity,  $\Gamma$  is the retardance,  $\theta$  is the projection of the LC director along the input window of the LC cell (twist angle), and  $a$  is the flicker amplitude. We note that  $\text{sinc}(a) \equiv \sin a/a$ . From the different parameters, in this work we are interested in the retardance  $\Gamma$ , which can be obtained by applying,

$$\Gamma = \arctan \left( \frac{\sqrt{S_1^2 + S_2^2}}{-S_3} \right) \quad (2)$$

The arctangent function is responsible for producing a wrapped phase result. This, together with the square root in the numerator generates an ambiguity in the resultant retardance  $\Gamma$  of  $180^\circ$ , as we will show in Fig. 2. As a physical guide for a robust phase unwrapping what we do is to simulate the expected retardance for a simplified LC cell filled with a commercial LC. To this goal we consider the well-known E7 compound, whose properties, such as its ordinary and extraordinary refractive indices for several wavelengths can be found in the literature [14].

We note that the vendors do not provide any information dealing with the LC material used in their devices or the thickness of the LC layer. In general, the thickness is the minimum necessary to achieve a  $360^\circ$  phase dynamic range in the spectral range specified for a particular LCoS, since this is accompanied by a faster LC time response (this depends on the quadratic inverse of the LC layer thickness). Then, apart from specific LCoS models intended for high retardance, the thickness in modern devices for the visible is about  $3 \mu\text{m}$  [2]. With all these assumptions, in line with the specifications of the PA-LCoS device under test in this work, which is designed for the visible, we calculate the retardance. We have done this for the wavelengths 473, 532 and 633 nm, sampling the visible spectrum. Then, we calculate the ratio between the retardance for 473 and 633 nm with respect to 532 nm, since this provides a magnitude that is not dependent on the layer thickness. Then, these simulated ratios will help us decide what is the number of multiples of the basic ambiguity step, in our case  $180^\circ$ , that is needed for the experimental ratios to have a physical sense. The retardance  $\Gamma$  is given by,

$$\Gamma = \frac{2\pi}{\lambda} d (n_{eff} - n_o) \quad (3)$$

, and  $\lambda$  is the illumination wavelength,  $d$  is the cell gap,  $n_o$  is the ordinary refractive index of the liquid crystal and  $n_{eff}$  is the effective refractive index described by,

$$n_{eff} = \frac{n_o n_e}{\sqrt{(n_o \cos \phi)^2 + (n_e \sin \phi)^2}} \quad (4)$$

, where  $n_e$  is the extraordinary refractive index of the liquid crystal, and  $\phi$  is the angle of the director axis (optical axis) of the LC molecules with respect to the traversing light beam direction. We consider perpendicular incidence, therefore in a PA-LCoS microdisplay the angle  $\phi$  is equal to the tilt angle, which increases with the applied voltage since the LC director axis tends to align with the applied electric field. The latter points perpendicular to the windows of the device. A rigorous modelling needs to consider that there is a pretilt angle established by the alignment layer coated on the inner side of the display windows. This makes that when no voltage is applied, the angle  $\phi$  is equal to this pretilt angle, with typical values between 5-10 degrees. Then, when the voltage is applied, the tilt of the molecules is not homogeneous along the cell thickness since the molecules in the vicinity of the alignment layer cannot tilt. The tilt is also not homogeneous in the transversal direction, due to fringing-field effects. However, to get a rough yet useful estimate, in what follows we will consider a homogeneous alignment across the LC cell. We will see that this is consistent to a large extent on the experimental results that we will show.

### 3. SIMULATED AND EXPERIMENTAL RESULTS

Previously we have discussed the modelling of the PA-LCoS microdisplay as a homogeneous LC layer and using the values of the refractive indices for the commercial compound E7. In this Section we will show the simulated and the experimental results obtained. In Fig. 1(a) we plot the simulated retardance as a function of the tilt angle  $\phi$  for wavelengths 473, 532 and 633 nm, considering a cell thickness of 3  $\mu\text{m}$ . This is the unwrapped retardance since we are applying Eq. (3) to calculate the values. We note that PA-LCoS are filled with nematic LC materials whose director axis corresponds to the slow axis of the LC molecules [2]. Then, in Fig. 1(a), the retardance values show the relative advance of light linearly polarized perpendicular to the LC director with respect to the one polarized parallel to it. The largest retardance corresponds to zero tilt, which is when no voltage is applied. Then, the increase in the applied voltage leads to a nonlinear decrease of the retardance. In Fig. 1(b) we show the ratios for 473 and 633 nm with respect to 532 nm as a function of the tilt angle. We see in the figure that for a homogeneous LC layer, the ratios have a very small dependence on the tilt angle. If we look at Eq. (3), the ratios are independent of the cell thickness, thus they represent a constraint imposed by LC materials. Then, this can be used to verify the goodness of unwrapped experimental retardance.

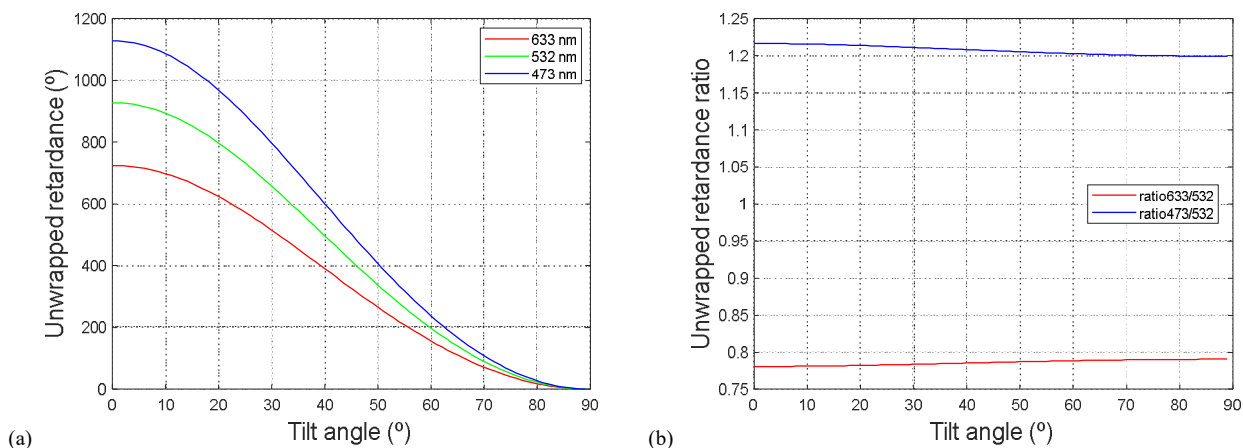


Figure 1. Simulated values for LC compound E7 and layer thickness 3  $\mu\text{m}$ . (a) Retardance, and (b) retardance ratios.

The commercial PA-LCoS microdisplay under test in this work is the model PLUTO for the visible spectral range, distributed by the company HOLOEYE. Its backplane is digitally addressed [15] and different pulse width modulation (PWM) addressing schemes (digital addressing sequences) can be generated by the driver electronics [15,16]. We consider the 5\_6 sequence format, where the first number indicates the quantity of “equally weighted” bit-planes, and the second number the quantity of “binary” bit-planes [15,16]. This sequence generates many addressing levels,  $(5+1) \times 2^6=384$  levels, with a reasonably low flicker magnitude. The two levels of the binary voltage signal across the LC layer can be set with the vendor software: the low and the high values are respectively the dark  $V_d$  and the bright  $V_b$  voltages. The best voltage choices for spatial light modulation correspond to using the lowest possible  $V_d$  value, since this reduces the flicker, and then increasing the value for  $V_b$  so that the needed retardance dynamic range is achieved [15]: typically

360° in most phase-only modulation applications. The lowest value for  $V_d$  needs to be over 0.5 Volts, since there is a threshold below which the molecules do not tilt [2,12]. The two voltage-pairs ( $V_d, V_b$ ) considered in this work are  $V_1=(0.56,1.55)V$  and  $V_2=(0.69,4.85)V$ , chosen to show the results when the voltage difference is not very high, and when this is almost the maximum difference available with the software. Also, we will see that changing the low level  $V_d$  from close to the threshold to a slightly larger value produces a clearly different starting retardance point.

In Fig. 2(a) and (b) we show respectively for the voltage-pairs  $V_1$  and  $V_2$ , the experimental results for the wrapped phase for the three wavelengths as a function of the gray level. The experimental measurement and characterization procedure is the one given in Ref. [7]. In these plots, we see that the retardance definition range is between  $-90^\circ$  and  $+90^\circ$ , i.e.  $180^\circ$ . We also see that there are  $180^\circ$  phase jumps and slope sign changes at the curve extrema. The number of phase jumps and extrema is larger in the case of voltage-pair  $V_2$  since the retardance range is larger than for  $V_1$ . The retardance should have a monotonous increasing (or decreasing) continuous behavior. Taking this physical principle, we design an algorithm that can stitch the different patches together and correct the slope sign changes at the extrema. With this, we get a continuous retardance curve but there is still an ambiguity of multiples of  $180^\circ$  in assigning the correct offset so that the retardance is the true one.

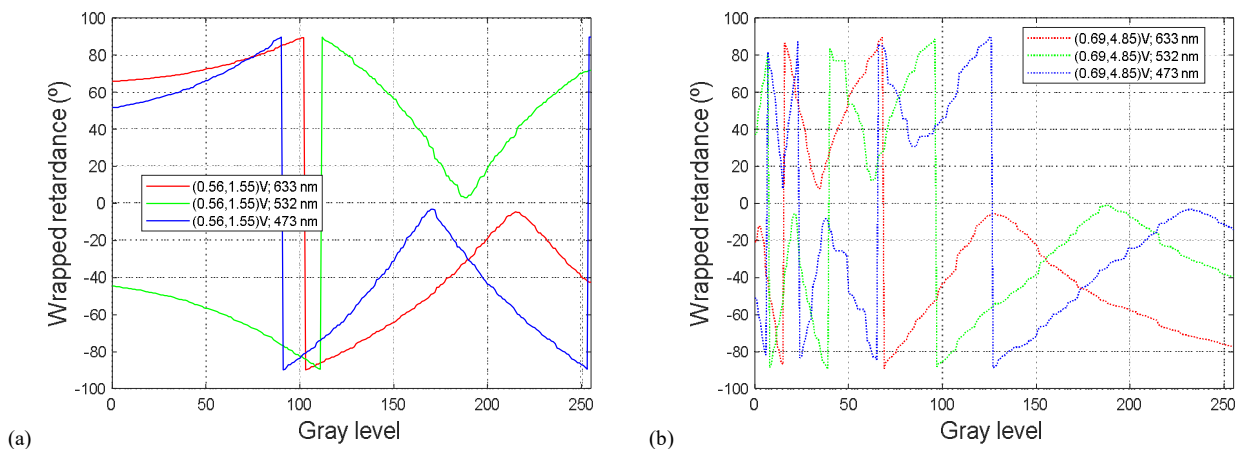


Figure 2. Wrapped experimental retardance values for the three wavelengths, for (a) voltage-pair  $V_1$ , and (b) voltage-pair  $V_2$ .

In Fig. 3(a) and (b) we show respectively the unwrapped retardance and the wavelength-related ratios for the experimental measurements shown in Fig. 2. In Fig. 3(a) we see that for the voltage-pair  $V_1$  the retardance range is clearly smaller than for  $V_2$ . In the latter, we see that the voltage dynamic range is clearly larger than  $360^\circ$ . We also see, that when comparing each wavelength for the two voltage-pairs, the case  $V_2$  starts at a lower retardance at gray level 0. As the gray level increases, the different bits in the sequence start turning to the on-state, and the whole accumulated voltage experienced by the LC molecules increases. In principle, the effective voltage experienced by the LC molecules is related with the root-mean square (RMS) voltage value along the image frame [15,16]. Then, with the gray level increase, the LC director reorients along the normal of the LC cell, i.e. its tilt angle increases as explained in Fig. 1. We see that the retardance variation with the gray level is not linear, and that it exhibits a saturation behavior in the case of curves for the voltage-pair  $V_2$  for larger gray levels, where the retardance is getting closer to zero.

In Fig. 3(b) we see the retardance ratios associated with the retardance curves given in Fig. 3(a). We have tried different combinations of retardance offsets for the three wavelengths and only one of them is providing ratios consistent with the ones obtained from the simulations with the E7 compound in Fig. 1(b). We see that the experimental ratios produce larger variations as a function of the gray level, especially for  $V_2$ , when compared with the plots in Fig. 1(b). This is probably due to non-homogeneous distribution of the LC director along the axial and the transversal directions of the LC layer, as discussed at the end of Section 2. We even see for the curves at  $V_2$  the jumps at some gray levels indicating the activation of a new bit in the digital sequence. The non-homogeneous 3D distribution of the LC director needs rigorous numerical simulation approaches to be evaluated, as shown by Francés et al. [10]. However, we have shown that a homogeneous approximation to estimate the wavelength retardance ratios suffices for the absolute unwrapping purposes in this work.

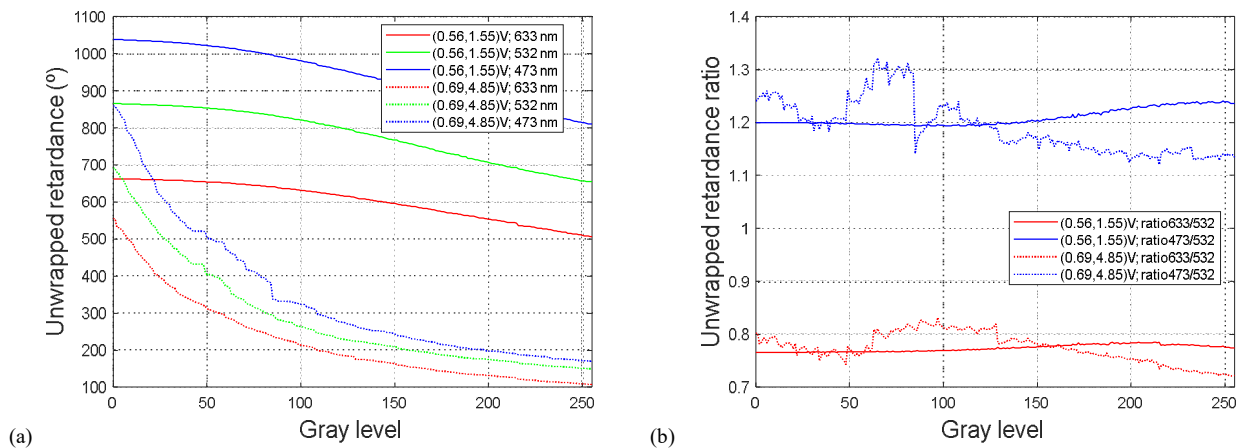


Figure 3. For the 3 wavelengths and for the 2 voltage-pairs, (a) unwrapped experimental retardance, and (b) wavelength ratios.

## 4. CONCLUSIONS

We have demonstrated a procedure to obtain the absolute unwrapped retardance of a PA-LCoS device. To this goal, we use the simulated values of the retardance ratios between different wavelengths in the visible. These simulations are based on the refractive indices for a commercial LC material, the E7 compound, typically found in the literature. This absolute calibration can be useful for some applications such as in spatial light modulation of the state of polarization (where  $180^\circ$  of ambiguity leads to confusing the slow and the fast axis of a retarder) or if we want to get a deeper insight into the details of the liquid crystal layer. The absolute retardance values obtained and their retardance ratios have shown how the retardance depends on the values for the two voltage levels in the binary signals addressed in digital backplane LCoS devices.

## ACKNOWLEDGEMENTS

Funded by the “Generalitat Valenciana” (Spain) (IDIFEDER/2021/014, cofunded by EU through FEDER Programme; and PROMETEO/2021/006), “Ministerio de Ciencia e Innovación” (Spain) (PID2021-123124OB-I00, PID2019-106601RB-I00). ARS-M thanks the “Generalitat Valenciana” for the grant (GRISOLIAP/2021/106).

## REFERENCES

- [1] Z. Zhang, Z. You, and D. Chu, “Fundamentals of phase-only liquid crystal on silicon (LCOS) devices,” *Light Sci. Appl.* 3, 1-10 (2014).
- [2] G. Lazarev, P.-J. Chen, J. Strauss, N. Fontaine, A. Forbes, “Beyond the display: Phase-only liquid crystal on Silicon devices and their applications in photonics,” *Opt. Express* 27, 16206–16249 (2019).
- [3] A. Márquez, A. Lizana, “Special Issue on Liquid Crystal on Silicon Devices: Modeling and Advanced Spatial Light Modulation Applications,” *Appl. Sci.* 9, 3049 (2019).
- [4] F. J. Martínez-Guardiola, A. Márquez, S. Gallego, J. Francés, I. Pascual, and A. Beléndez, “Retardance and flicker modeling and characterization of electro-optic linear retarders by averaged Stokes polarimetry,” *Opt. Lett.* 39, 1011-1014 (2014).
- [5] J. García-Márquez, V. López, A. González-Vega, and E. Noé, “Flicker minimization in an lcos spatial light modulator,” *Opt. Express* 20 (2012).
- [6] H. Yang and D. P. Chu, “Phase flicker optimisation in digital liquid crystal on silicon devices,” *Opt. Express* 27 (2019).

- [7] A. Márquez, F. J. Martínez-Guardiola, J. Francés, E. M. Calzado, D. Puerto, S. Gallego, I. Pascual, and A. Beléndez, "Unitary matrix approach for a precise voltage dependent characterization of reflective liquid crystal devices by average stokes polarimetry," *Opt. Lett.* 45, 5732-5735 (2020).
- [8] B. Apter, U. Efron, and E. Bahat-Treidel, "On the fringing-field effect in liquid-crystal beam-steering devices," *Appl. Opt.* 43 (2004).
- [9] C. Lingel, T. Haist, and W. Osten, "Optimizing the diffraction efficiency of slm-based holography with respect to the fringing field effect," *Appl. Opt.* 52 (2013).
- [10] J. Francés, A. Márquez, C. Neipp, D. Puerto, S. Gallego, I. Pascual, and A. Beléndez, "Polarimetric analysis of cross-talk phenomena induced by the pixelation in pa-lcos devices," *Opt. Laser Technol.* 152, 108125 (2022).
- [11] F. J. Martínez, A. Márquez, S. Gallego, J. Francés, I. Pascual, and A. Beléndez, "Effective angular and wavelength modeling of parallel aligned liquid crystal devices," *Opt. Lasers Eng.* 74, 114–121 (2015).
- [12] A. Márquez, F. J. Martínez-Guardiola, J. Francés, S. Gallego, I. Pascual, A. Beléndez, "Combining average molecular tilt and flicker for management of depolarized light in parallel-aligned liquid crystal devices for broadband and wide-angle illumination," *Opt. Express* 27, 5238-5252 (2019).
- [13] R. Li and L. Cao, "Progress in Phase Calibration for Liquid Crystal Spatial Light Modulators," *Applied Sciences* 9, 2012 (2019).
- [14] J. Li, C.-H. Wen, S. Gauza, R. Lu, and S.-T. Wu, "Refractive indices of liquid crystals for display applications," *J. Disp. Technol.* 1, 51–61 (2005).
- [15] F. J. Martínez, A. Márquez, S. Gallego, M. Ortuño, J. Francés, A. Beléndez, and I. Pascual, "Electrical dependencies of optical modulation capabilities in digitally addressed parallel aligned liquid crystal on silicon devices," *Opt. Eng.* 53 (2014).
- [16] A. Hermerschmidt, S. Osten, S. Krüger, T. Blümel, "Wave front generation using a phase-only modulating liquid-crystal based micro-display with HDTV resolution," *Proc. SPIE* 6584, 65840E (2007).